

# SSMIS 1D-VAR RETRIEVALS

Godelieve Deblonde

*Meteorological Service of Canada, Dorval, Québec, Canada*

## Summary

Retrievals using synthetic background fields and observations for the SSMIS (Special Sensor Microwave Imager Sounder) instrument were obtained with the SSMIS1DVAR\* (one-dimensional variational assimilation scheme) for non-precipitating skies over the oceans. Two retrieval techniques are implemented in the 1D-Var. Technique a is based on Phalippou (1996). With technique b, the natural logarithm of total water content (sum of specific humidity and liquid cloud water content) is a control variable. The impact of removing biases between the observed and forward modeled brightness temperatures is illustrated with technique a. It is also shown that in the presence of clouds, little temperature information can be extracted using technique a if the a priori cloud position is not well known. With technique b, temperature information can be extracted from the observations because it has some skill at positioning the cloud.

\*The SSMIS1DVAR is software developed by the NWP Satellite Application Facility. The bulk of the SSMIS1DVAR Version 1 software was developed by the author, in collaboration with S. J. English, as a visiting scientist at the Met Office.

## 1. Introduction

A stand-alone one dimensional variational assimilation scheme (1D-Var) was developed to compute retrievals from DMSP (Defense Military Satellite Project) SSMIS (Special Sensor Microwave Imager/Sounder) brightness temperatures ( $T_b$ 's). The SSMIS (scheduled for launch in October 2002) was designed to measure profiles of humidity, temperature, surface properties such as marine surface wind speed and cloud liquid water path.

The 1D-Var scheme can be solved in cloudy but non-precipitating atmospheres using two different techniques. Technique a is based on Phalippou (1996). His scheme, originally designed for the DMSP SSM/I (Special Sensor Microwave Imager), retrieves profiles of natural logarithm of humidity ( $\ln q$ ), surface wind speed ( $SWS$ ) and liquid water path ( $LWP$ ). In the implementation of his method for the SSMIS, retrievals of temperature ( $T$ ) profiles were also added. Technique b, retrieves profiles of natural logarithm of total water content (sum of specific humidity  $q$  and cloud liquid water contents  $q_L$ ) and profiles of  $T$  and  $SWS$ . An empirical function governs how the total water content ( $q_{total}$ ) is split among its components. Cloud water is formed when the atmospheric relative humidity ( $RH$ ) reaches a pre-set threshold value. Technique b has similarities to that presented in Rosenkranz (2001) for the NOAA AMSU-A/-B instruments (Advanced Microwave Sounding Unit). Blankenship et al. (2000) also presented a somewhat similar retrieval scheme, for humidity profiles only, that uses SSM/I integrated water vapor ( $IWV$ ) (obtained from a regression equation) and the  $T_b$ 's of the SSM/T-2 (DMSP microwave moisture sounder) 183 GHz channels.

The retrieval results presented here used the SSMIS channels with weighting functions that peak below 0.1 hPa and are listed in Table 1. One of the main reasons for using simulated data is that it allows for a thorough testing and a more complete understanding of the retrieval scheme.

Table 1 SSMIS Channel Parameter Specification (provided by B. Burns, Aerojet).

Channel #	Center Freq. (GHz)	1 <sup>st</sup> IF, 2 <sup>nd</sup> IF, bandwidth* per pass band (MHz)	Polarization	NeΔT (K) for 305 K Scene*	(E+F) <sup>1/2</sup> (K)
1	50.3	0.,0.,380.	H	0.21	1.5
2	52.8	0.,0.,388.8	H	0.2	0.4
3	53.596	0.,0.,380.	H	0.21	0.4
4	54.4	0.,0.,382.5	H	0.20	0.4
5	55.5	0.,0.,391.3	H	0.22	0.4
6	57.29	0.,0.,330.	H+V	0.26	0.4
7	59.4	0.,0.,238.8	H+V	0.25	0.4
8	150.	1250.,0.,1642.	H	0.53	3.0
9	183.31	6600.,0.,1526.	H	0.56	3.0
10	183.31	3000.,0.,1019.	H	0.39	3.0
11	183.31	1000.,0.,512.5	H	0.38	3.0
12	19.35	0.,0.,355.0	H	0.35	2.4
13	19.35	0.,0.,356.7	V	0.34	1.27
14	22.235	0.,0.,407.5	V	0.45	1.44
15	37.0	0.,0.,1615.	H	0.26	3.00
16	37.0	0.,0.,1545.,	V	0.22	1.34
17	91.655	900.,0.,1418.	V	0.19	1.74
18	91.655	900.,0.,1411.	H	0.19	3.75
22	60.792668	357.892,5.5,2.62	H+V	0.58	0.64
23	60.792668	357.892,16.,7.32	H+V	0.37	0.46
24	60.792668	357.892,50.,26.5	H+V	0.38	0.47

\*Measured for this unit prior to launch

## 2. 1D-Var methodology

The a priori or background information of the atmosphere and surface ( $x^b$ ), and the measurements  $y^o$  (observed  $Tb$ 's) are combined in a statistically optimal way to obtain an estimate of the most probable atmospheric state  $x$ . Gaussian error distributions (with zero mean) are assumed for both  $x^b$  and  $y^o$  and it is also assumed that the background and observation errors are uncorrelated. The most probable state is obtained by minimizing the cost function  $J(x)$  (e.g. Lorenc 1986).  $J(x)$  may be written as:

$$J(x) = \frac{1}{2}(x - x^b)B^{-1}(x - x^b)^T + \frac{1}{2}(y^o - H(x))(E + F)^{-1}(y^o - H(x))^T \quad (1)$$

$B$ ,  $E$  and  $F$  are respectively, the background, the instrument, and the representativeness (includes forward modeling errors) error covariance matrices. The superscripts T and -1 denote transpose and inverse respectively.  $H(x)$  is the observation operator which here is the fast radiative transfer model RTTOV Version 6.7. This version uses the fast surface emissivity model FASTEM2 (English and Hewison 1998, Deblonde and English 2000) and was adapted by the author for the SSMIS instrument. The Levenberg-Marquardt technique is used to find the minimum of the cost function.

For technique b, the control vector consists of a profile of  $T$  (at 43 levels  $\leq 0.1$  hPa), a profile of  $\ln q_{total}$  (at 22 levels  $< 200$  hPa) and  $SWS$ .  $q$  depends on  $q_{total}$  as follows (Fig. 1): Let  $RH_{q_{total}} = q_{total}/q_{sat}$ , and constants  $RH_1=0.95$ ,  $RH_2=1.05$  and  $C_{split}=0.5$ , where  $q_{sat}$  is the specific humidity at saturation. Then for

$$\begin{aligned} RH_{q_{total}} < RH_1 : \quad q &= q_{total} \\ RH_2 > RH_{q_{total}} \geq RH_1 : \quad q &= RH_1 q_{sat} + C_{split} [q_{total} - RH_1 q_{sat}] \\ RH_{q_{total}} \geq RH_2 : \quad q &= q_{sat} (RH_1 + C_{split} (RH_2 - RH_1)) \end{aligned} \quad (2)$$

and  $q_L = q_{total} - q$ . Thus, once  $RH_{q_{total}}$  reaches a threshold value of  $RH_1$ , the excess of  $q_{total}$  over  $RH_1 q_{sat}$  is split among  $q$  and  $q_L$ . When  $RH_{q_{total}}$  exceeds  $RH_2$ , then  $q$  remains fixed and the excess is taken by  $q_L$ .

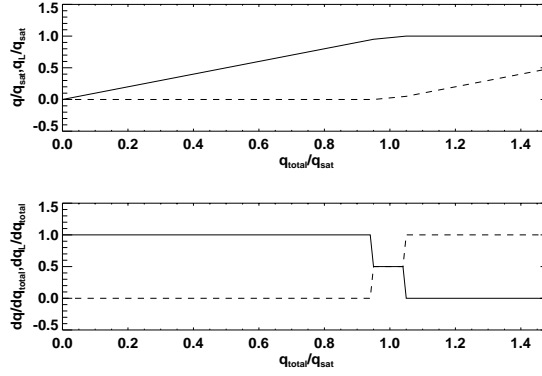


Figure 1 **a)** Dependence of  $q/q_{sat}$  and  $q_L/q_{sat}$  on  $q_{total}/q_{sat}$  ( $q_{total}=q+q_L$ ). **b)** Derivatives of  $q$  and  $q_L$  with respect to  $q_{total}$  as a function of  $q_{total}/q_{sat}$ . The continuous line illustrates  $q$  and the dashed line  $q_L$ .

Retrievals were performed with simulated background fields  $x^b$  and simulated brightness temperatures  $Tb^o$  (or  $y^o$  above) as in Eyre (1989). A sample size  $N$  of 3000 was used. Two true profiles ( $x^{true}$ ) were selected: the US standard atmosphere and a tropical atmosphere ( $IWV$  of respectively 14.2 and 41.3  $\text{kgm}^{-2}$ ). Both profiles had  $SWS = 7 \text{ ms}^{-1}$  which is roughly the globally averaged surface wind speed over the oceans. In technique a, where cloud water was added to the true profiles,  $q$  was replaced by its saturated value. All background fields contained the same cloud as the true profile. For technique b, where cloud water was added,  $q$  was saturated to only  $RH_1$  to avoid formation of cloud by this saturation step (Eq. 2). This step was followed by the addition of the cloud and  $q_{total}$  was computed. The latter was then split among  $q$  and  $q_L$ . Clouds in the background fields were determined using the splitting functions (Eq. 2) and varied from one profile to another since noise (see below) was added to the true profile of  $\ln q_{total}$ .

The background error covariances for profiles of  $T$  and  $\ln q$ , air temperature at 2 m,  $\ln q$  at 2 m were obtained from the Met Office 1D-Var background error data set for two latitude bands: 30°S-30°N or TR and 30°N-90°N or NH. Covariances between  $T$  and  $\ln q$  or  $\ln q_{total}$  were set to zero (univariate analysis). For  $SWS$  background error, a value of  $2 \text{ ms}^{-1}$  was used. For technique a, the  $LWP$  background error was set to  $0.2 \text{ kgm}^{-2}$ . Such a large error value implies that the  $LWP$  is unconstrained by the background. For technique b,  $\ln q_{total}$  was assigned the same background error as  $\ln q$ . The background error of the atmospheric pressure at 2 m was set to 1 hPa for all cases.

Values of  $(E+F)^{1/2}$  are listed in Table 1. The errors for channels 12 to 18 (SSM/I like channels) and channels 8 to 11 (similar to SSM/T-2) were taken from (Deblonde 2001) and are based on observation minus forecast (6h forecast  $Tb$ 's computed with RTTOV) statistics of  $Tb$ 's. For the remaining channels, error estimates are based on English (1999).

The normalized computed error (NCE) is defined as:

$$NCE = \frac{SD(x^{sol} - x^{true})}{B_i^{1/2}} \quad (3)$$

where the superscript sol refers to the 1D-Var solution. For a given  $y = x_1 - x_2$ , Bias ( $x_1 - x_2$ ) and SD ( $x_1 - x_2$ ) are defined as follows:

$$Bias(y) = \frac{1}{N} \sum_{i=1}^N y_i \quad (4)$$

$$SD(y) = \sqrt{\frac{1}{N-1} \sum_{i=1}^N (y_i - \bar{y})^2} \quad (5)$$

### 3. Results

The 1D-Var was solved with technique a using as true profile the cloudless tropical profile with NH background errors (Experiment NCa1, a list of experiments is provided in Table 2). With the background and observation errors as specified, a very low value of NCE (0.16) was obtained for  $IWV$  and indicates a very large impact of the observations since the solution error is much lower than the background error. Several of the SSMIS window channels (low optical depth) are very sensitive to  $IWV$ . As shown in Fig. 2b, Bias( $lnq^{sol} - lnq^{true}$ ) is not zero for all heights but Bias( $IWV^{sol} - IWV^{true}$ ) for NCa1 is small ( $0.08 \text{ kgm}^{-2}$ ).

In the 1D-var formulation used here, it is assumed that the background error of  $lnq$  follows a Gaussian distribution. Hence the corresponding background error distribution of  $q$  is not Gaussian and is skewed. If one simplifies the 1D-Var problem by assuming that  $lnq$  is retrieved at a single level, then

$$\ln q^b = \ln q^{true} + N(0, \sigma_b^2) \quad (6)$$

and it can be shown that the mean of  $q^b$  over the ensemble of profiles is given by:

$$\langle q^b \rangle = q^{true} e^{\sigma_b^2/2} \quad (7)$$

where  $\langle \dots \rangle$  indicates an ensemble mean. For  $\sigma_b=0.5$ , which is a typical value of  $lnq$  background error, this corresponds to a mean bias of 13% for  $q^b$  with respect to  $q^{true}$ . This is why Bias( $IWV^b - IWV^{true}$ ) is not zero.  $IWV$  is related to  $q$  via a linear operator. Bias( $IWV^b - IWV^{true}$ ) for NCa1 is  $3.15 \text{ kgm}^{-2}$ .

For the US standard true profile experiment (relatively dry profile), biases between the observations and the forward model  $Tb$ 's (computed from the background fields) or  $\langle Tb^o - Tb(x^b) \rangle$  were computed when it was assumed that either the background error distribution of  $lnq$  is Gaussian or that of  $q$  is Gaussian. For the latter case,  $B(lnq)$  was first converted to  $B(q)$ . Mean, variance and skewness of the distribution of  $Tb^o - Tb(x^b)$  for these assumptions are listed in Table 3 for the moisture sensitive window channels. The variances of  $Tb^o - Tb(x^b)$  for both cases are close, indicating that both distributions have a similar variability as is required for the intercomparison to be valid. The distribution of  $Tb^o - Tb(x^b)$  is considerably more Gaussian (lower values of skewness and visual inspection of the distributions) if the background errors of  $q$  are assumed Gaussian rather than those of  $lnq$ . This is due to a more linear dependence for the window channels of  $Tb$  on  $q$  rather than  $lnq$ . When the same assumption is made with the true tropical profile (larger non-linear dependence of  $Tb$  on moisture), the same conclusion applies but only for the few most transparent channels.

Table 2 List of Experiments. NH background errors were used for all experiments.

Experiment	Retrieval Tech.	True Profile	Clouds in true profile	Cloud Top/ Bottom pressure (hPa)/ - LWP ( $\text{kgm}^{-2}$ )	Comment

Nca1	A	Tropical	No		bias not removed
Nca2	A	Tropical	No		bias removed
Ca3	A	US Standard	Yes	700/750/0.3	CSF* from BG cloud
Ca4	A	US Standard	Yes	700/750/0.3	CSF from BG RH
Ca5	A	US Standard	Yes	750/950/0.5	CSF from BG cloud
Ca6	A	US Standard	Yes	750/950/0.5	CSF from BG RH
Cb7	B	Tropical	Yes	750/950/0.19	
Cb8	B	Tropical	Yes	700/750/0.27	

\*BG= Background, CSF= Cloud Structure Function, RH=Relative Humidity.

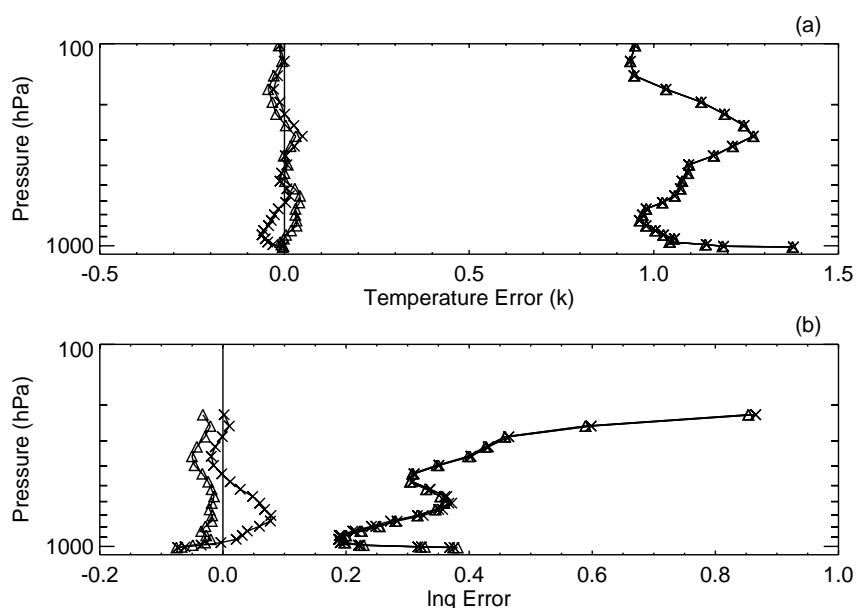


Figure 2 Temperature and  $\ln q$  profile retrieval errors for a cloudless true tropical profile with NH background errors for Experiment Nca1 (no bias removed --triangles) and Nca2 (bias removed --X signs). **a)** Bias ( $T^{\text{sol}} - T^{\text{true}}$ ) is on the left of the figure and SD ( $T^{\text{sol}} - T^{\text{true}}$ ) on the right. **b)** same as in **a)** but for  $\ln q$ .

Table 3  $Tb^o - Tb(x^b)$  statistics for choosing either a Gaussian distribution for background error of  $\ln q$  (first entries) or  $q$  (second entries). US standard atmosphere with NH background errors.

SSMIS Channel #	Mean	Variance	Skewness
1	-0.67, -0.17	3.24, 2.82	-0.95, -0.093
12	-1.57, -0.16	20.42, 19.86	-0.78, 0.029
13	-0.82, -0.091	5.68, 5.48	-0.800, 0.016
14	-1.61, 0.0146	22.14, 23.93	-0.57, 0.18
15	-1.38, -0.32	13.56, 11.87	-0.96, -0.092
16	-0.657, -0.156	3.10, .70	-0.97, -0.10
17	-1.23, -0.22	12.83, 12.58	-0.605, 0.127
18	-3.43, -0.57	94.03, 93.108	-0.59, 0.144

Before computing the retrievals, one may remove the biases computed above ( $\langle Tb^o - Tb(x^b) \rangle$  with background errors of  $\ln q$  assumed Gaussian) for each channel as is done in an operational context (e.g Harris and Kelly 2001). Experiment Nca1 was re-executed but with biases removed first. Retrieval results for this experiment

(NCa2) are illustrated in Fig. 2. The SD of  $T$  and  $lnq$  hardly changed but the bias in  $IWV^{sol}$  changed from 0.083 to 2.419  $\text{kgm}^{-2}$  and the bias of  $IWV^b = 3.153 \text{ kgm}^{-2}$  is closer to that of  $IWV^{sol}$ . However, a bias in  $SWS$  and  $LWP$  retrievals have now also been introduced. As shown in Fig. 2, removing the bias in  $Tb$ 's has not eliminated the bias of  $lnq$  as a function of height. The bias correction has changed the mean retrieved value of  $IWV$  while the redistribution of  $IWV$  with height is controlled both by the background error statistics and the non-linear dependencies of  $Tb$  on  $lnq$ . The non-linearity of the problem increases with the size of the background errors. Only the 150 GHz channel and channels that sample the 183 GHz water vapor absorption line do humidity sounding for the tropical profile here in question. Furthermore, the maximum sensitivity of the 183 GHz channels to humidity is considerably less than that of the window channels. All the other humidity sensitive channels are window channels that sense integrated humidity and therefore do not provide much information on its vertical distribution.

With technique a, the impact of the a priori knowledge of cloud position was tested. With this technique, only  $LWP$  is solved for. The cloud structure function ( $CSF$ ) defined as  $q_L^b/LWP^b$ , which determines the cloud position, remains constant during the minimization (to find the minimum of Eq. 1). For synthetic retrievals, it is also assumed that the background cloud is always the true one. Since the  $LWP$  background error was set to a large value, the retrieved  $LWP$  will be different for each sample since Gaussian noise was added to the observations.

With retrievals of real observations, a cloud is not always present in the background and to allow cloud formation, the  $CSF$  has to be non-zero for at least one level. When there is no cloud in the background field, a non-zero  $CSF$  is created at levels where the  $RH$  profile exceeds a preset threshold value. If the  $RH$  of the given background profile does not exceed the specified threshold at any of the levels, then a non-zero  $CSF$  is created for the 3 levels above 975 hPa. Several levels are introduced to help with smoothness of jacobians.

To illustrate the impact of the knowledge of the cloud position (thus  $CSF$ ) using synthetic retrievals, the  $CSF$  was obtained solely with the two approaches listed in the above paragraph. This allows for cloud be formed in the wrong position. This experiment was tested for two cloud types: (A)  $LWP$  0.3  $\text{kgm}^{-2}$  situated between 700 and 750 hPa and (B)  $LWP=0.5 \text{ kgm}^{-2}$  situated between 750 and 950 hPa. For experiments with cloud type A (Ca3 –control and Ca4 test case), retrieval results in Fig. 3 show that when the knowledge of cloud position is not good then very little temperature information can be obtained from the observations. However, retrievals for other variables such as the  $lnq$  profile,  $IWV$  and  $SWS$  are only slightly deteriorated. This points to the independence between the temperature and the other variables. For the deeper and heavier cloud case, cloud type B, (Ca5—control and Ca6 –test case), the retrievals are affected in a similar way as for the cloud type A experiment (Fig. 3).

Thus, with technique a, if the a priori cloud position is not well known, little temperature information (except well above the cloud) is to be expected in cloudy skies, while the retrievals of the other fields are reasonably accurate.

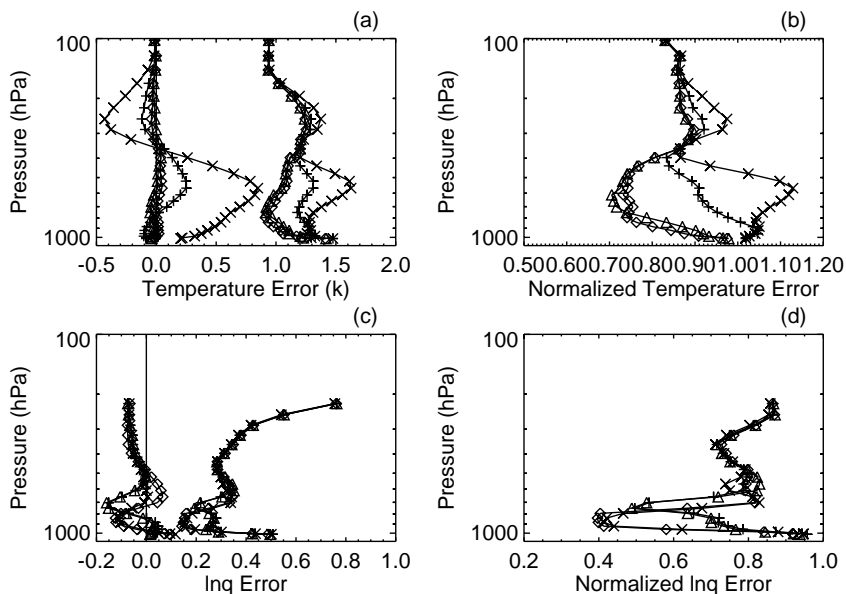


Figure 3 Effect of knowledge of a priori cloud position. Temperature and  $\ln q$  profile retrieval errors for a cloudy true US standard profile with NH background errors for Experiments Ca3 and Ca5 (with CSF from background cloud or control cases) and Ca4 and Ca6 (with CSF from background RH or test cases). Triangles are used for Ca3, plus signs for Ca4, diamonds for Ca5 and X signs for Ca6. In **a)** and **c)** Bias is on the left of the figure and SD on the right. **b)** Temperature Normalized Computed Error, **d)**  $\ln q$  Normalized Computed errors.

Fig. 4 illustrates retrieval statistics for experiments with technique b for two different cloud types and for a tropical profile with NH background errors. Cb7 has a thicker true cloud (750 to 950hPa) than Cb8 (700 to 750 hPa) and the  $LWP$  values are respectively  $0.19 \text{ kgm}^{-2}$  and  $0.27 \text{ kgm}^{-2}$ . The  $LWP$  amounts are different from technique a experiments because of the way clouds are generated (Eq. 2). As for the cloudless true profile case, not all sample profiles converge (divergence percentage for Cb7 = 24% and Cb8 = 18%) and the number of diverging cases is substantially larger ( $\sim 10\%$  for cloudless cases). As a result, the sample set is incomplete and statistics are available for only a subset of the ensemble of profiles. Nevertheless, the solutions are similar to those obtained with technique a (compare Fig. 3 experiments Ca3 and Ca4 and those of Fig. 4). However, with technique b, a CSF did not have to be used and it is possible to retrieve temperature even in the presence of clouds (Fig 4 b). As for technique a, where large biases in  $\ln q$  were found at cloud height (Fig. 3c), large biases in  $\ln q_{total}$  are also generated at cloud height with technique b (Fig. 4c). Fig. 5 illustrates histograms of retrieved  $LWP$  for Cb7 and Cb8. The  $LWP$  tends to be overestimated and a few cases have large retrievals of  $LWP$ . Most of these cases correspond to cases with cloud formation at the surface which are mitigated with technique a. This could also be done for technique b.

## 4. Conclusions

Retrievals using synthetic background fields and observations were investigated for the SSMIS instrument for non-precipitating conditions over the oceans. The main reasons for using synthetic data was to verify the correctness of the implementation of the 1D-Var scheme and to investigate the behavior of retrievals using a new technique. Also, at this time, the SSMIS instrument is scheduled for launch in the fall.

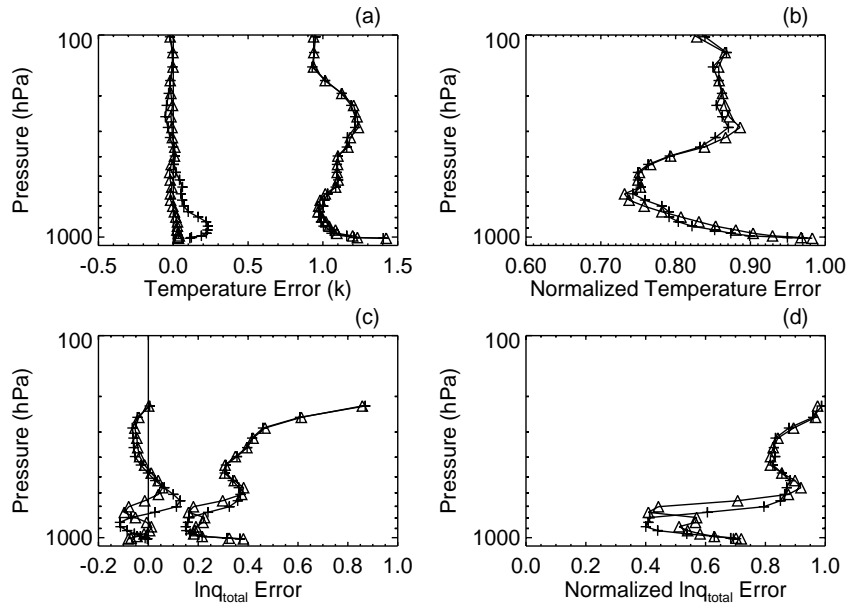


Figure 4 Same statistics as in Fig. 3 but for Experiments Cb8 (triangles) and Cb7 (plus signs). The true profile is the tropical profile with NH background errors are used.

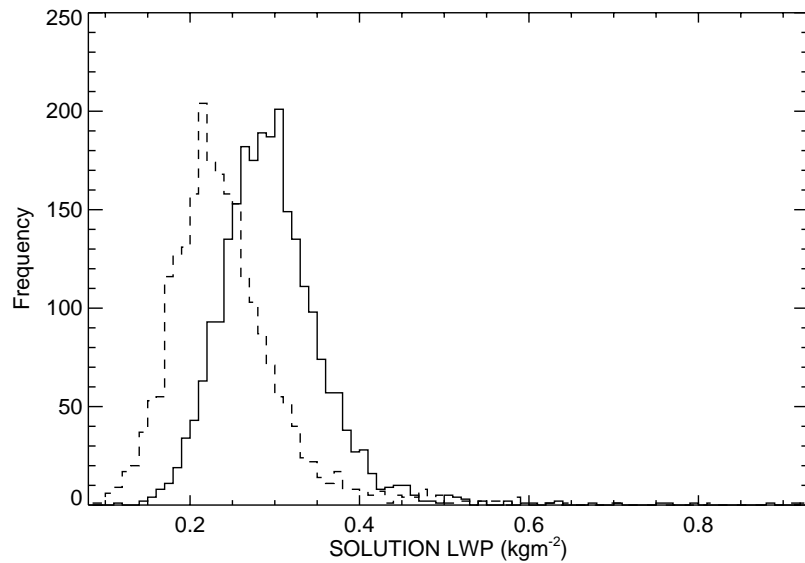


Figure 5 Histograms of cloud liquid water path ( $\text{kgm}^{-2}$ ) for Experiments Cb8 (continuous line) and Cb7 (dashed line).

Two retrieval techniques were implemented in the 1D-Var and were extensively tested. The control variables for the two techniques were the same except for the following: in technique a, profiles of  $\ln q$  and  $LWP$  are control variables and, in technique b,  $\ln q_{total}$  is a control variable where  $q_{total}$  is the sum of specific humidity and liquid cloud water content. Functions were also defined that specify how  $q_{total}$  is split among its two components. Essentially, excess water vapor over saturation leads to cloud formation.

First, the impact of removing biases between the observed and forward modeled  $Tb$ 's was discussed. Secondly, for cloudy true profiles, it was shown that little temperature information (except well above the clouds) can be extracted with technique a if the a priori cloud position is not well known. Technique b however, allows for some temperature retrieval from the observations because it has some skill at positioning



the cloud. This is the main advantage of using technique b. This comes at a cost though by considerably increasing the number of iterations before convergence of the minimization problem is reached and a considerable number of cases do not converge.

## 5. References

Blankenship, C. B., A. Al-Khalaf and T. T. Wilheit, 2000: Retrieval of water vapor profiles using SSM/T-2 and SSM/I data. *J. Atmos. Sciences*, **57**, 939-955.

Deblonde, G. and English, S.J., 2000: Evaluation of the fastem2 fast microwave oceanic surface emissivity model, Technical Proceedings of the 11th International ATOVS Study Conference, Budapest, Hungary, 20-26 September 2000.

Deblonde, G. 2001: Variational Retrievals Using SSM/I and SSM/T-2 Brightness temperatures in Clear and Cloudy Situations. *J. Atmos. Oceanic Tech.*, **18**, 559-576.

English, S.J. and T.J. Hewison, 1998: A fast generic millimeter-wave emissivity model. Proc. *SPIE*, **3503**, 288-300.

English, S.J., 1999: Estimation of temperature and humidity profile information from microwave radiances over different surface types. *J. Appl. Meteorol.*, **38**, 1526-1541.

Eyre J.R., 1989: Inversion of cloudy satellite sounding radiances by nonlinear optimal estimation. I: Theory and simulation for TOVS, *Q.J.R. Meteorol. Soc.*, **115**, 1001-1026.

Harris, B.A. and G. Kelly, 2001: A satellite radiance-bias correction scheme for data assimilation, *Q.J. R. Meteorol. Soc.*, **127**, 1453-1468.

Lorenc, A.C., 1986: Analysis methods for numerical weather prediction. *Q. J. R. Meteorol. Soc.*, **112**, 1177-1194.

Phalippou, L., 1996: Variational retrieval of humidity profile, wind speed and cloud liquid-water path with the SSM/I: Potential for numerical weather prediction. *Q.J.R. Meteorol. Soc.*, **122**, 327-355.

Rosenkranz, P.W., 2001: Retrieval of temperature and moisture profiles from AMSU-A and AMSU-B measurements., *IEEE Trans. Geoscience Remote Sensing*, **39**, 2429-2435.